ELSEVIER

Magnetotelluric studies in Puga valley geothermal field, NW Himalaya, Jammu and Kashmir, India

T. Harinarayana[*], K.K. Abdul Azeez, K. Naganjaneyulu, C. Manoj, K. Veeraswamy, D.N. Murthy, S. Prabhakar Eknath Rao

National Geophysical Research Institute, Hyderabad-500 007, India

Abstract

Puga geothermal field in NW Himalaya, Ladakh district, Jammu and Kashmir, India, is situated near the junction of the Indian and Asian plates. The thermal activity is attributed to the widespread igneous activity during Upper Cretaceous to late Tertiary age. The study area located at an altitude of 4600 m above mean sea level is characterized by springs with temperatures up to 84 °C that correspond to the boiling point of water at this altitude. In order to image the shallow and deeper parts of the area, wideband (1000–0.001 Hz) magnetotelluric (MT) measurements have been carried out. Five-component MT data were acquired from the E–W-trending, 15-km-long and 1-km-wide Puga valley at 35 locations. The data have been subjected to one- (1D) and two-dimensional (2D) modelling. The results confirm the presence of a shallow conductive region in the area and also indicate the presence of a deep conductive region (5–15 Ω m) commencing from a depth of about 1.5 to 2.0 km and related to the presence of a geothermal reservoir.
© 2004 Elsevier B.V. All rights reserved.

Keywords: magnetotellurics; geoelectrical modelling; geothermal field; Puga valley; Himalaya

1. Introduction

Puga valley is one of the major geothermal provinces in Himalayan belt region and represents one of the most extensive hot spring activities in India. The area is located in Ladakh district of Jammu and Kashmir, India, in the NW Himalayas and situated at an altitude of about 4400 m above mean sea level with surrounding hills rising up to an altitude of about 6000 m. Puga valley is well known for its numerous hot springs with temperatures up to 84 °C (the boiling point of water at that altitude) and occurrences of sulfur and borax deposits (Ravishankar et al., 1976). The valley trends in almost E–W direction, between Sumdo Village in the east and Polokongka La in the west, over a stretch of about 15 km with a maximum width of about 1 km (Fig. 1).

---

* Corresponding author. Tel.: +91 40 23434613; fax: +91 40 27171564.

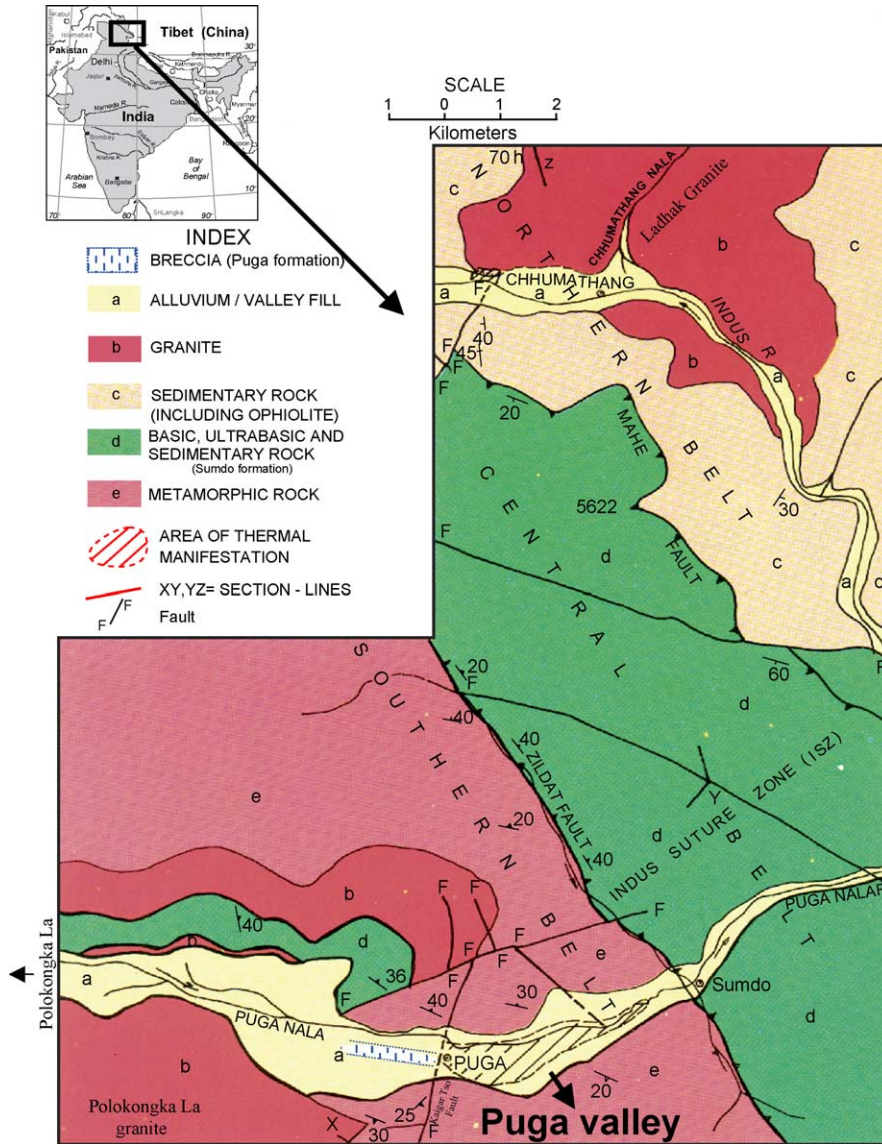*E-mail address:* tharinarayana@hotmail.com (T. Harinarayana).

Fig. 1. Geology and tectonic map of Puga and surrounding region (modified from Geothermal Atlas of India, 1991).

The Puga area lies adjacent to the south of the Indus Suture Zone (ISZ) which has been believed to be a major crustal subduction zone, confirmed by the discovery of blue schist facies from its basic rocks by Virdi et al. (1977). The valley appears to be a down faulted block with its northern and southern faults concealed under the valley material, that consists of recent to subrecent deposits of glacial morains, eolian sand, clay and scree. Borax and sulfur, which are genetically connected with thermal fluids, occur widely in the eastern part of the valley.

Geophysical exploration for the subsurface geothermal reservoir was started in early 1980, mainly employing shallow electrical resistivity surveys (Arora et al., 1983). These experiments as well as the geological and geochemical investigation could successfully establish the existence of geothermal anomaly and the presence of shallow reservoir

features (Chowdhury et al., 1974; Gupta et al., 1975; Arora et al., 1983; Singh et al., 1983; Mishra et al., 1996). While shallow structure of the region is well explored with geological, geophysical and even with shallow boreholes (<400 m) (Gupta et al., 1975; Arora et al., 1983, Singh et al., 1983; CEA, 1995; Mishra et al., 1996), the deep structure need to be explored for the delineation of source of the geothermal anomaly using an efficient geophysical tool.

The magnetotelluric (MT) method is the most appropriate electromagnetic technique to electrically image the subsurface structures. In geothermal regions, it can provide useful information about the lateral and vertical variation of the resistivity of subsurface. Magnetotelluric transfer functions are calculated from measurements of horizontal electric and magnetic fields at the surface of the Earth and can image the subsurface electrical resistivity (Cagniard, 1953). Because of the skin depth effect of electromagnetic fields, the high-frequency MT transfer function carries information about the shallow resistivity structure of the Earth, whereas the low-frequency transfer function carries information about the deeper structure (Vozoff, 1991). The present magnetotelluric sounding study in this area is aimed to bring out the electrical structure of the shallow as well as deeper parts to delineate anomalous structure, if any, related to the geothermal activity.

2. Brief geology and tectonics of the area

The Puga geothermal field lies close to and south of the 'Indus Suture Zone', and represents the collision junction of the Indian and the Asian plates that were involved in the Himalayan orogeny. This zone was subjected to intense basic to ultrabasic, plutonic to submarine volcanism of Cretaceous age (ophiolites) and several phases of wide spread acid igneous activity from Upper Cretaceous to Upper Tertiary. The ophiolite suite of rocks, seen along the Indus suture zone, represents the remnants of the uplifted wedge of the oceanic crust.

Three distinct tectonic belts separate the area around Puga geothermal field in the upper Indus valley (Fig. 1). The northern tectonic belt comprises of sedimentary rocks belonging to Indus group and lie unconformably over the Ladhakh Granites. The

central belt, described as the 'Indus Suture Zone' is characterized by a large thickness of basic, ultrabasic and sedimentary rocks. This belt is bounded by Mahe fault in the north and Zildat fault in the south. The southern belt consists of a large thickness of sedimentaries, metasedimentaries and metamorphics intruded by at least two phases of granitic activity. The general direction of tectonic transport and intensity of metamorphism increases from north to south as a result of which rocks exposed in the southern belt are highly deformed and exhibit medium to high-grade metamorphism.

The Puga geothermal field is a part of the southern tectonic belt (Fig. 1), bounded on either side by prominent faults, characterized by volcanic sedimentary assemblages. The Puga valley is covered by recent and subrecent deposits of glacial moraines and eolian sand and scree, which are encrusted with borax, sulfur and other hotspring deposits. This loose valley-fill material continues up to 15–65 m depth range. Thereafter, hard reconsolidated breccia continues up to the depth of the basement rock (paragneisses and schists) known as Puga formation of probable Paleozoic age (Raina et al., 1963; Baweja, 1967). The basement rock is intruded by Polokongka La granite in the west. While in the east, the Sumdo formations are exposed. The thermal manifestations are confined to eastern part of the 15-km valley and are broadly aligned along the faulted crest of an anticline in the Puga formation. To the west of the area of thermal manifestations, a regional fault crosses the valley. This fault (Kaigar Tso fault) broadly delimits the thermally anomalous area on the western side. Zildat fault (Fig. 1) seems to be eastern limit of the thermal manifestations. Along the base of the northern hills in the central portion of the valley sulfur condensates are found and it probably represent an old line of fumarolic activity along a hidden fault (?) (Ravishankar et al., 1976).

3. Geothermal manifestations

The high heat flow density values obtained in the thermal surveys have established the existence of thermal anomaly in the valley. Over 100 hot springs with temperatures varying from 35 to 84 °C occur in the Puga valley with discharge rate up to 5 l/s

(Ravishankar et al., 1976). On the basis of the inferred subsurface thermal conditions, the valley is divided into two parts. The first part is characterized by low (normal for the location of the valley) subsurface temperature and other part is characterized by abnormal surface and subsurface temperature. The hot springs, hot pools, sulfur and borax deposits have been found in an area of 3 km^2 along a 4-km-long stretch of the eastern part of the valley where anomalous temperature observations are made. Shallow thermal data obtained in the valley showed that the observed shallow temperature gradients are positive in the eastern part of the valley. The temperature gradients are negative outside this zone, both towards the east and the west (Gupta et al., 1983). It is inferred that the anomalous near surface thermal conditions are caused by heat and mass transfer from shallow reservoir of estimated temperature of about 165 °C. During the course of an exploration for sulfur and borax by the Geological Survey of India during 1968–1970, a few boreholes yielded steam/hot water mixtures. It was considered that the shallow reservoir derives its heat mainly through hot water, which ascends probably from a deep-seated reservoir and flows underneath the valley through N–S and NE–SW lateral channels (Gupta et al., 1983).

4. Data acquisition and analysis

Wideband (8192 Hz to 1/4096 Hz) MT data acquisition units (GMS 05) of M/s Metronix were employed to measure the time varying components of Earth's electric (Ex, Ey) and magnetic fields (Hx, Hy, Hz). A total of 35 MT soundings were carried out within the valley (Fig. 2) in a grid fashion during June–July, 2001. In addition, two more MT measurements were made outside the valley (not shown in figure), towards the east of Sumdo village, in order to have picture about the eastern extension of geothermal field. The measurements were carried out for 24–36 h at each station in four frequency bands (8192–256, 256–8, 8–1/4 and 1/4–1/128 Hz) and 1/128 to 1/4096 Hz data is made by the digital filtering of band 4 data. As Puga Valley is uninhabited and far away from cultural noise sources, the recorded data were of very good quality. The lack of coherent noise sources and high predicted coherency between electric and mag-

netic channels justifies the single station recording. Time series segments with obvious disturbances (spikes and spurious data points) were discarded prior to processing. The time series subsections were tapered and Fourier transformed. Cross- and auto-spectra matrices of individual segments were computed after removing system response. Preferential stacking of the spectra matrices (Stodt, 1983) based on coherency yielded the final cross and auto spectra of field elements. Apparent resistivity, phase and variance were computed from these elements using Robust procedures (PROCMT User' guide, 1990). Fig. 3 shows the computed apparent resistivity and phase values plotted against frequency for few MT soundings from the valley.

5. Qualitative analysis of the data

The MT apparent resistivity curves from Puga valley can be grouped into three categories indicating the lateral changes in resistivity along the E–W direction. The MT curves from stations located in the western part of the valley forms the first category (Fig. 4a) and shows apparent resistivity in the range of 500–800 Ω m towards the high-frequency end (>100 Hz), increasing to about 1000 Ω m near 10 Hz. It gradually decreases to 10–100 Ω m at the lower-frequency end. The second category (Fig. 4b) is formed by curves from the central part of the valley and indicates that the apparent resistivity is in the range of 10–50 Ω m at the high frequencies (>100 Hz) followed by a gradual increase reaching 50–200 Ω m near 0.3 Hz. It gradually decreases to 1–50 Ω m at the low-frequency end. The third category (Fig. 4c), somewhat similar to the first category, is the group of curves from the extreme eastern side of the valley and shows a decrease in resistivity at lower frequency being rather gradual as compared to first category. These three categories of curves clearly indicate the lateral changes in resistivity along the valley and delineates the anomalous conductive region of the Puga valley where most of the Hot Springs are present. The semiquantitative analysis, using Bostick transformation (Bostick, 1977; Goldberg and Rotstein, 1982), of the MT data also confirms the lateral variation in resistivity at different depths with in the valley.
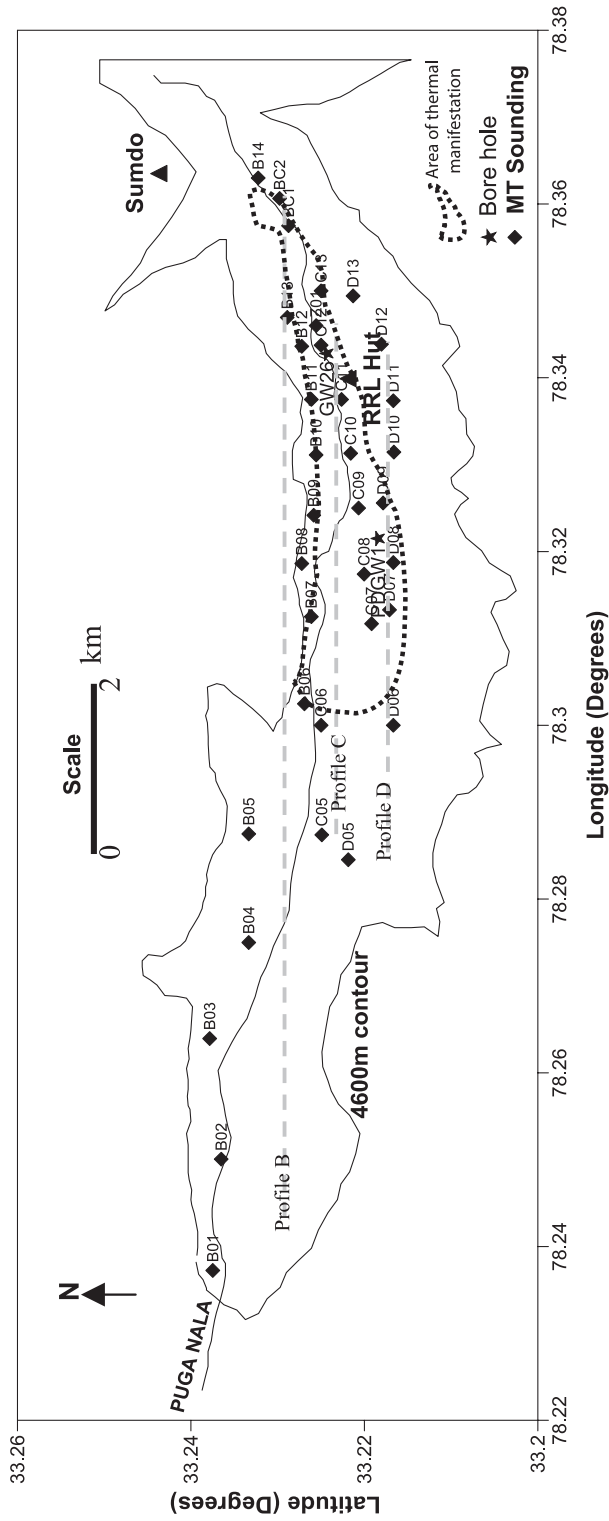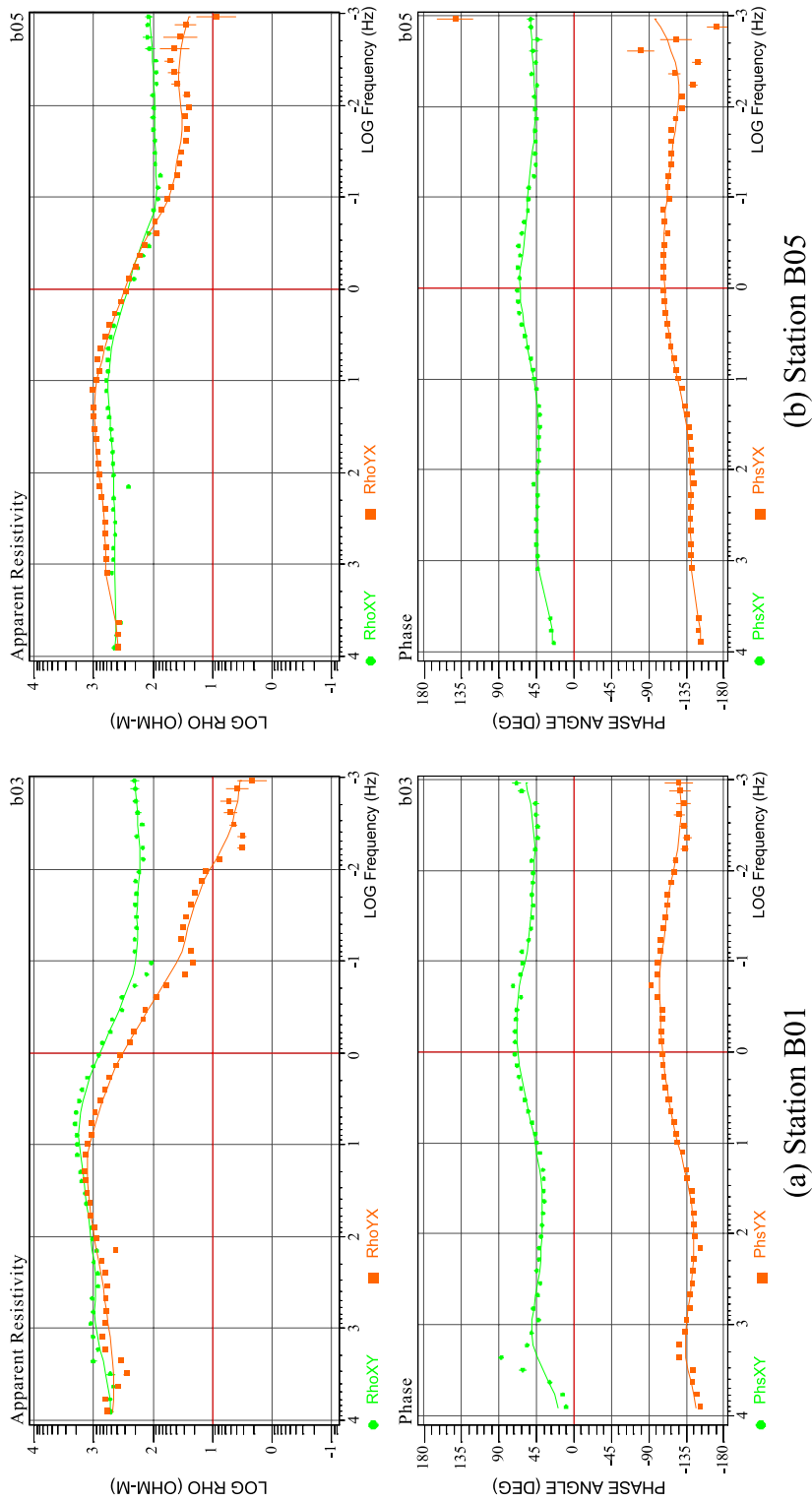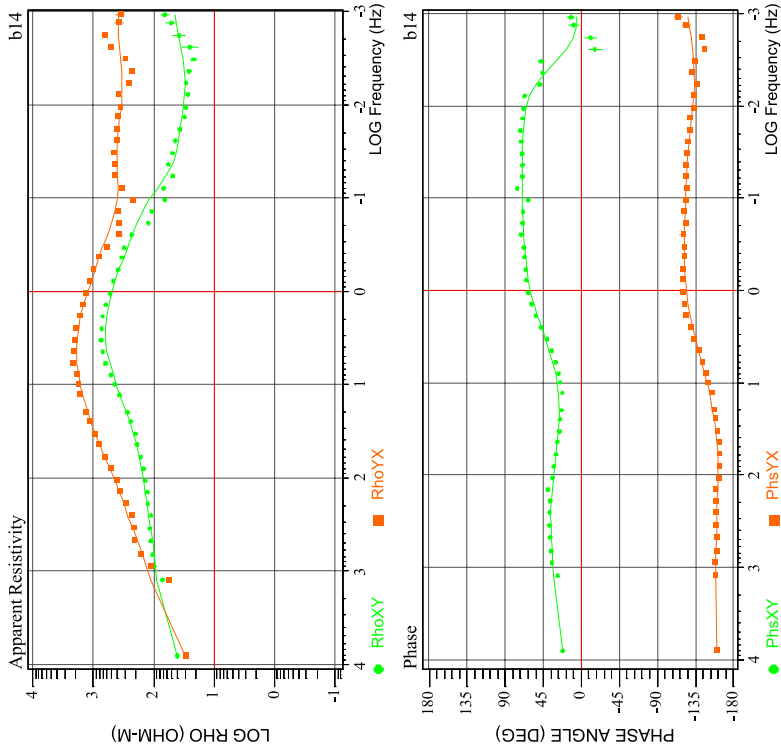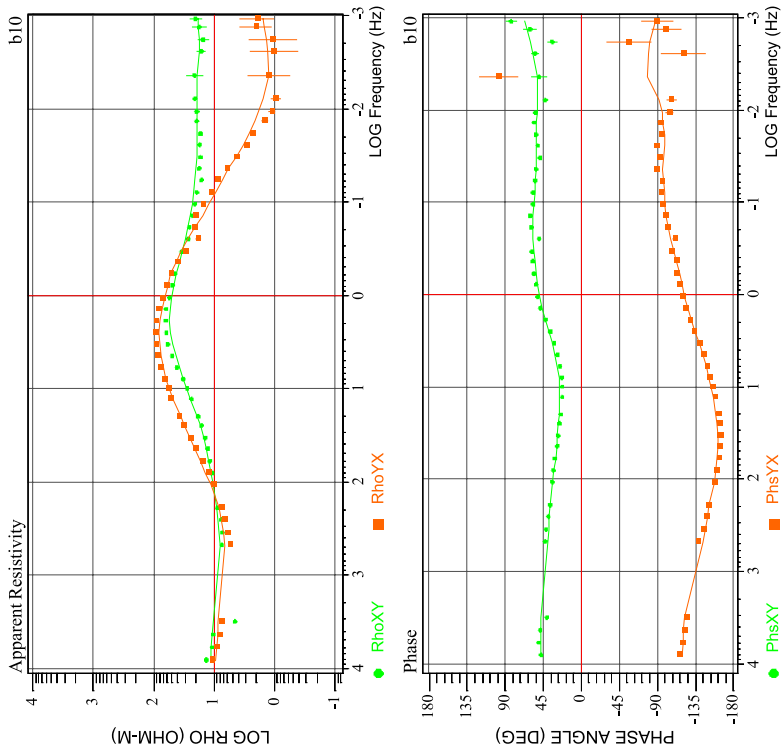
Fig. 2. Location map of MT soundings.

Fig. 3. Typical apparent resistivity (ρ_{xy} and ρ_{yx}) and phase curves (Φ_{xy} and Φ_{yx}).
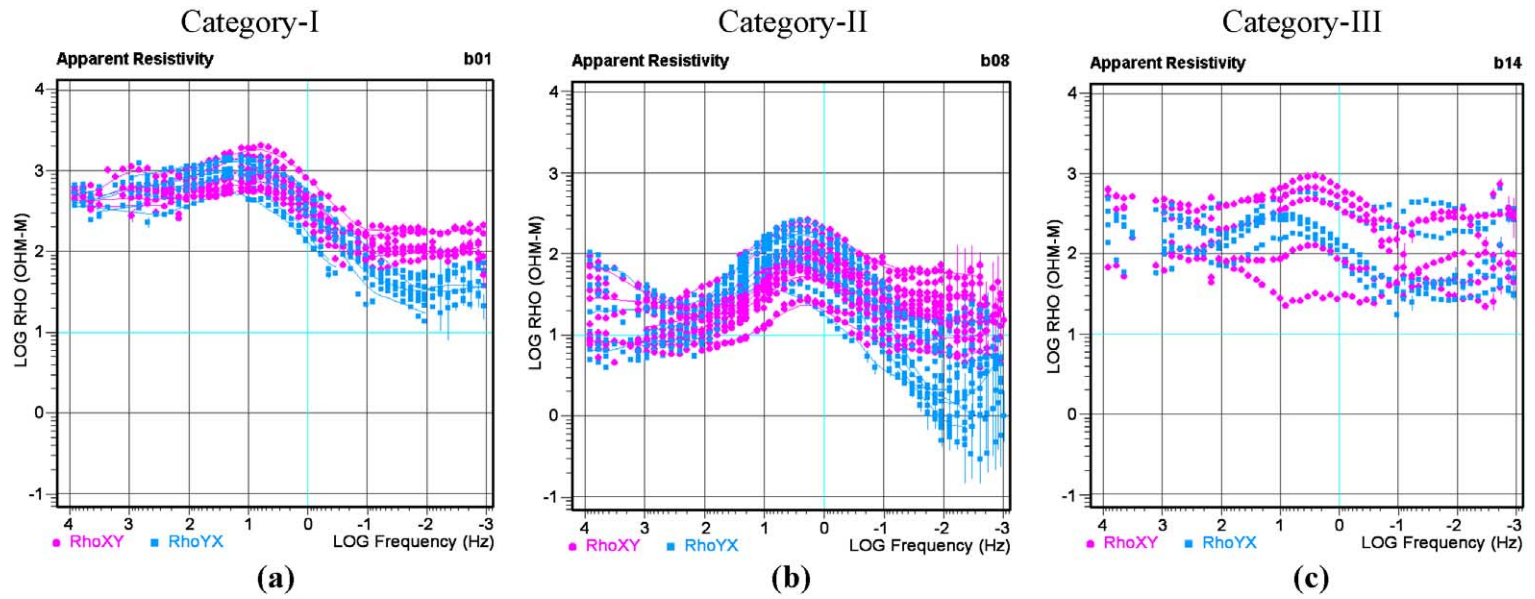
Fig. 3 (*continued*).

Fig. 4. Apparent resistivity curves from all the sites within Puga Valley grouped into three categories: panels a and c are from western and eastern sides of the valley and the anomalous curves in panel b are from the central part of the valley.

6. Induction arrows

The relations between the vertical and horizontal magnetic fields yield information about lateral resistivity variation. Induction arrows, constructed from magnetic transfer functions, indicate the direction and strength of the conductor as a function of frequency. The real part of the Parkinson induction arrow (Parkinson, 1962; Jones, 1986) with reversed angle points towards the direction of enhanced conductivity and it is plotted (Fig. 5) for a few representative stations located in Puga valley for four frequencies

(100, 10, 0.1 and 0.01 Hz). It can be seen from the figure (Fig. 5a and b) that the data at high frequencies (100 and 10 Hz) exhibit an evidence for the presence of enhanced conductivity in the region between profile B and profile D of Fig. 2. The induction arrows along profile B and profile D pointing each other, towards the centre of the valley (i.e., towards profile C) indicate the existence of shallow high conductive zone between these two profiles. This corroborates with the earlier geophysical studies carried out in the region by Geological Survey of India (GSI) and others (Gupta et al., 1975; Arora et
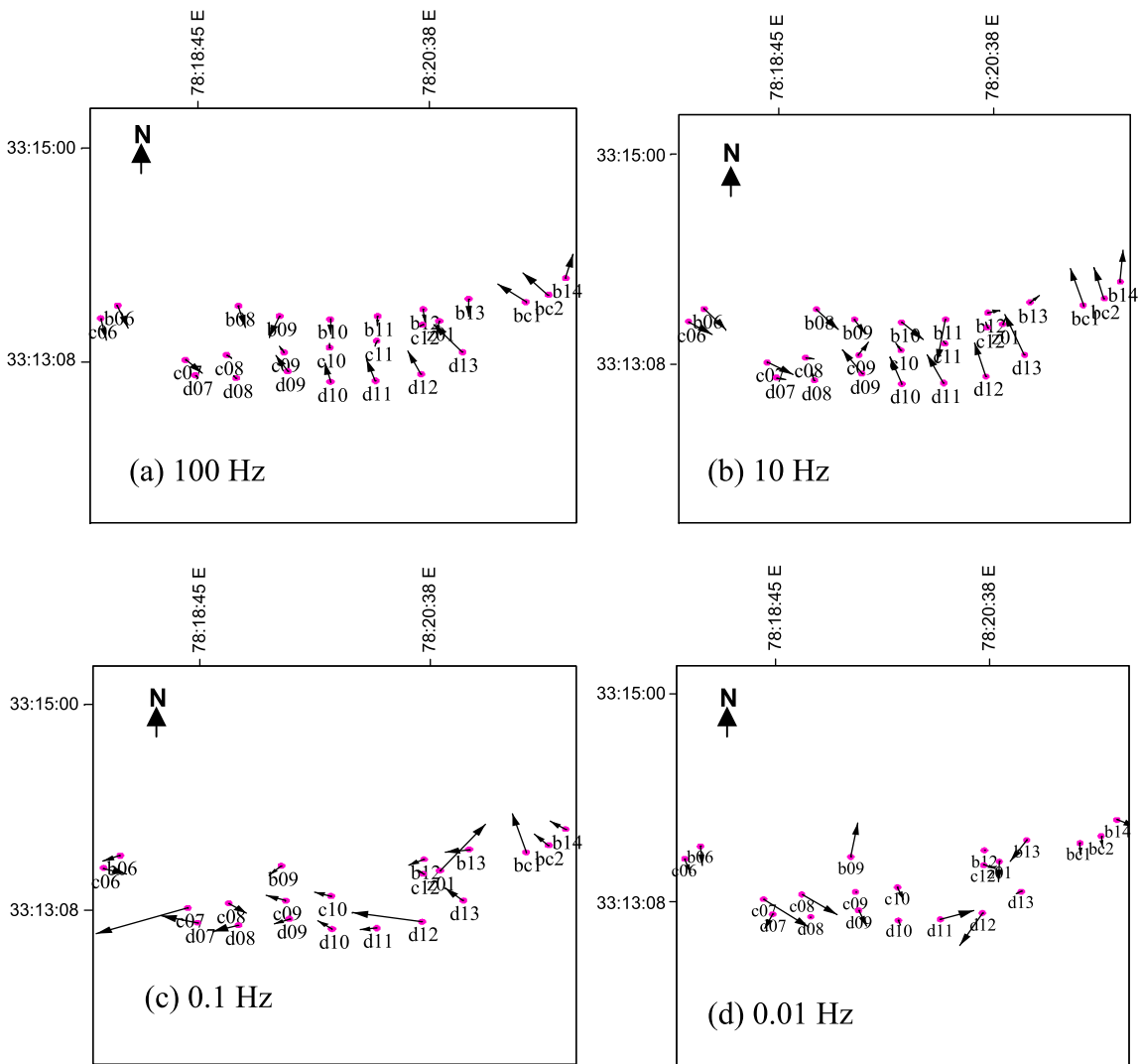

Fig. 5. Parkinson real induction arrows plotted for 4 frequencies: (a) at 100 Hz, (b) at 10 Hz, (c) at 0.1 Hz and (d) at 0.01 Hz.
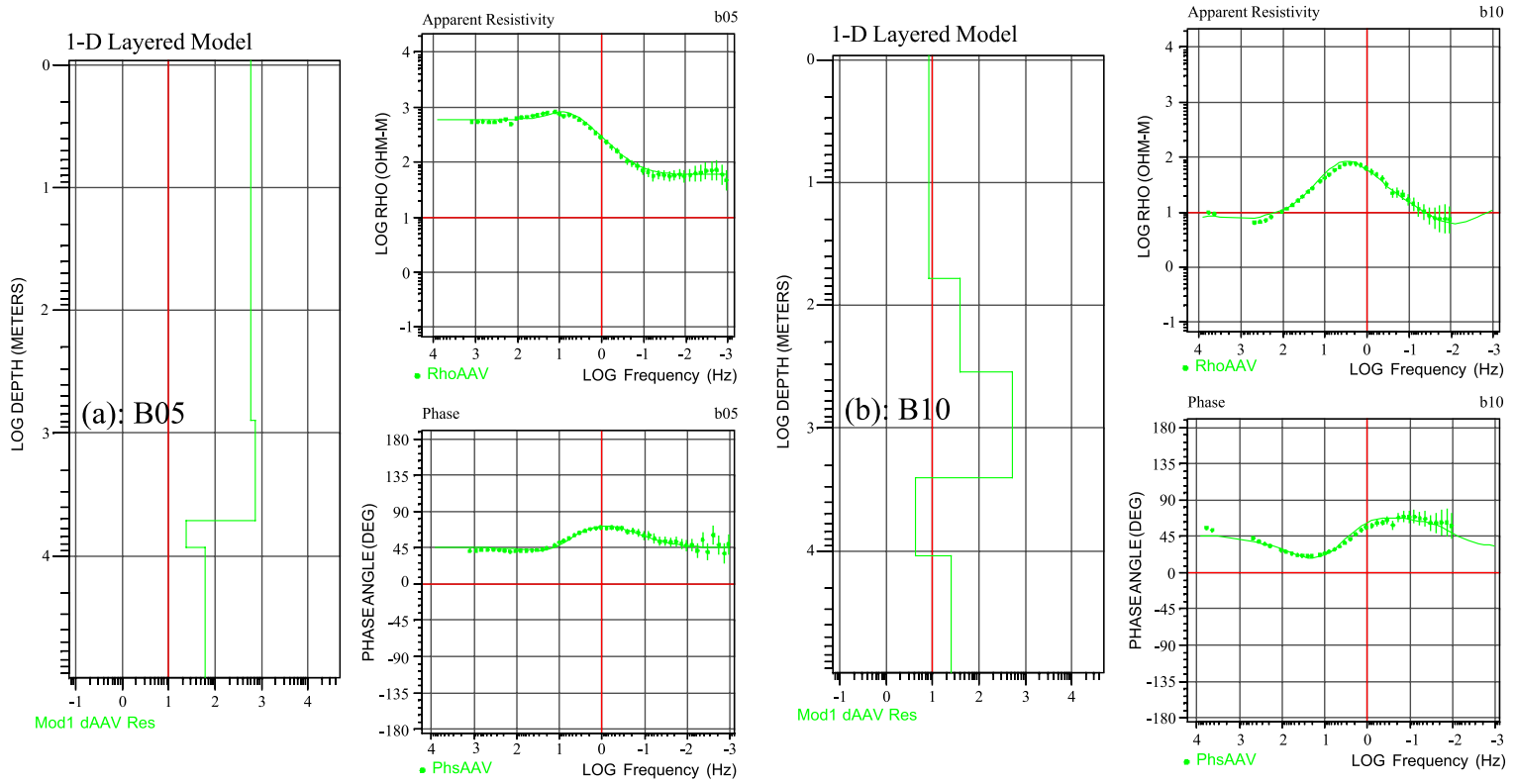
Fig. 6. 1D layered model based on Marquardt inversion for three representative stations: (a) B05, (b) B10 and (c) B14. Symbols in the right side show the measured values and continuous line indicate the model response.
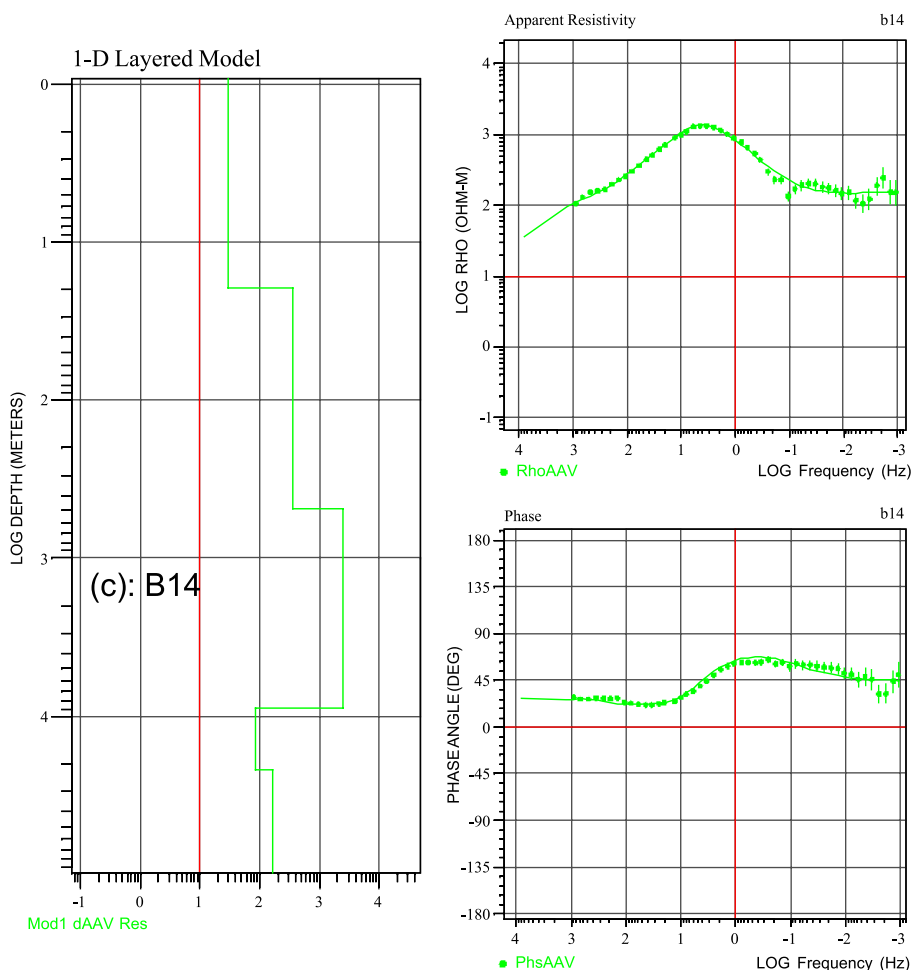
Fig. 6 (*continued*).

al., 1983; Singh et al., 1983; Mishra et al., 1996). Although induction arrows at lower frequencies (0.1 and 0.01 Hz) are not similar to high-frequency data, it shows the presence of enhanced conductivity at deeper level within the region (Fig. 5c and d).

7. Inversion of MT data

7.1. One-dimensional inversion

The application of 1D inversion schemes to the MT data is simple and fast enough in obtaining the resistivity distribution of horizontal layers as a function of depth for quantitative interpretation of MT data. As a preliminary step to 2D inversion, the effective average impedance (Berdichevsky and Dimitriev, 1976; Ranganayaki, 1984), which are rotationally invariant in the surface plane is used to generate 1D layered models. This average impedance data has been used to generate 1D layered earth model and found to provide useful results (Ingham and Hutton, 1982; Livelybrooks, 1986; Sule and Hutton, 1986) and works well with many 2D structures. One-dimensional (1D) inversion of the data was first carried out using Occam linearized inversion scheme (Constable et al., 1987) that includes a large number of layers and then that of Marquardt algorithm (Marquardt, 1963). The layered model from Marquardt inversion is presented in Fig. 6a to c, for the

representative stations (stations B05, B10 and B14) belonging to each category group curves. In Fig. 6a–c, the layered model is shown in the left side. In the upper right part of Fig. 6a–c, the symbol represent the measured apparent resistivity values and the continuous line indicate the model response. The symbol in the right bottom of the Fig. 6a–c represents the measured phase value and continuous line indicates the model response. The layered earth resistivity model for the station B05, located towards the western part of the valley (first category of curves) (Fig. 6a), shows a resistive top layer (600 Ω m) with a 800-m-thick and a more resistive (750 Ω m) layer underneath this layer. Beneath these resistive strata, the model shows the existence of a conductive layer (15 Ω m) at a depth of 5.5 km followed by a slightly higher resistive layer (60 Ω m). On the other hand, the station B10 located towards the anomalous part of the valley shows (Fig. 6b) that a conductive top layer (10–40 Ω m) of 260 m thickness is followed by a resistive layer (500 Ω m) up to a depth of about 3 km. Below this layer, an anomalous conductive (5 Ω m) layer continues up to about 10 km and then rises to 30 Ω m. The station B14 (Fig. 6c) from the east extreme part of the valley shows resistive top layers (500–2000 Ω m) extending upto the depth of about 8 km followed by a comparatively low resistive layers of 80–150 Ω m. The 1D inversion results of few MT stations is compared with the nearest borehole information available in the area and they show good agreement. The MT results of stations C09 and C12 are compared with the boreholes PDGW1 and GW26 of Fig. 2, respectively. The Table 1 shows the

comparison of the results. The drilling results showed that, in general, the top layer of valley consists of alluvium with varying thickness (15–200 m) underlain by breccia/bedrock. The drilling results from the deepest (384.7 m) borehole in the area, PDGW1, showed 130 m thickness of alluvium and other borehole GW26 of 60 m deep showed 36-m-thick alluvium layer (Jangi and Bajaj, 1992). Inversion results of station C09 shows a 121-m-thick surface layer of 8 Ω m corresponding to the alluvium followed by a 44 Ω m second layer corresponding to the fracture breccia/bedrock. The C12 station model gives a 39-m-thick top layer of 10 Ω m corresponding to the alluvium layer and a 39 Ω m second layer corresponding to fractured breccia/bedrock in the area.

7.2. 2D Inversion

Although 1D results, as described earlier, have provided basic quantitative information of subsurface structure, 2D modelling of the data provide better constraints on the model. After 1D inversion of the data, we applied the Rapid Relaxation Inversion (RRI) code of Smith and Booker (1991) to derive two-dimensional (2D) electric resistivity structure of the area. The RRI inversion approach determines the subsurface resistivity with least structure consistent with the data. The data in measured direction; XY (north–south) and YX (east–west) are rotated to the regional electric strike direction to orient the data into transverse electric (TE-parallel to strike) mode and transverse magnetic (TM-perpendicular to strike) mode. Regional electric strike is determined from Groom–Baily (Groom and Baily, 1989) single station analysis. Regional electric strike of N 40 °W is obtained at lower frequencies from Groom–Baily analysis (Fig. 7a–c) and shows good agreement between MT strike with the regional geological strike of the Puga and surrounding region. The static shift distortions have been corrected using statistical procedures (Jones, 1988). This has been carried out based on the local geology of the Puga valley region. It may be noted that the region is covered with alluvium of thickness ranging from 10 m to about 300 m at the centre of the Puga valley (Ravishankar et al., 1976) and the basement is exposed towards the western and eastern parts of the Puga valley. Statistical procedures

Table 1
Comparison of the characteristics of boreholes PDGW1 and GW26 with layered models obtained from 1D inversion of MT sites near them

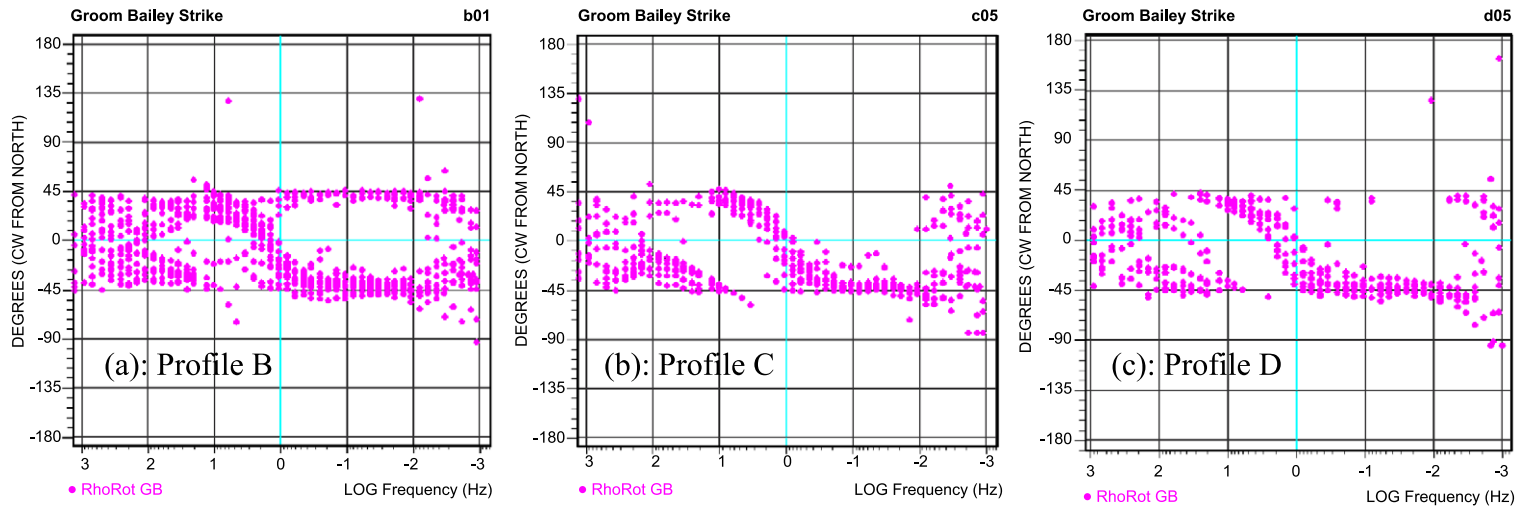| Bore hole information				Model parameters of first two layers from MT	
Bore hole no.	Drilled depth in m	Depth (in m) to bedrock/ breccia	Nearest MT station in m	Apparent resistivity in Ω m	Thickness in m
GW26	60	36	C12	10	39
				36	147
PDGW1	384.7	130	C09	8	121
				44	358

Fig. 7. Groom–Baily strike angle shown by the data set along (a) profile B, (b) profile C and (c) profile D.

are applied separately to each category of group for static shift correction of apparent resistivity data. The apparent resistivity variation along the profile B of Fig. 2 is shown in Fig. 8 before (top) and after correction of static shift (bottom).

Half space with a resistivity of 80 Ω m is assumed as initial model for the RRI inversion and the TE-mode and TM-mode data are jointly inverted for frequencies between 1000 and 0.001 Hz to derive a smooth subsurface electric structure. As described earlier, the data were acquired along three profiles only (profiles B, C and D) in the Puga valley (east–west). The rugged

topography of the Puga valley imposes constraints to plan more profiles across the valley (north–south). The insufficient data in the north–south direction makes it difficult to have a 2D model across the valley. Thus, 2D inversion along the three E–W-oriented profiles is carried out separately. Accordingly, subsurface sections obtained along these three profiles are presented in Fig. 9a (top), b (middle), and c (bottom), respectively. The subsurface electric image derived from 2D inversion indicate the presence of a common surface conductive (5–15 Ω m) zone (marked in Fig. 9a, b and c) with about 300–400 m thick at the centre of the
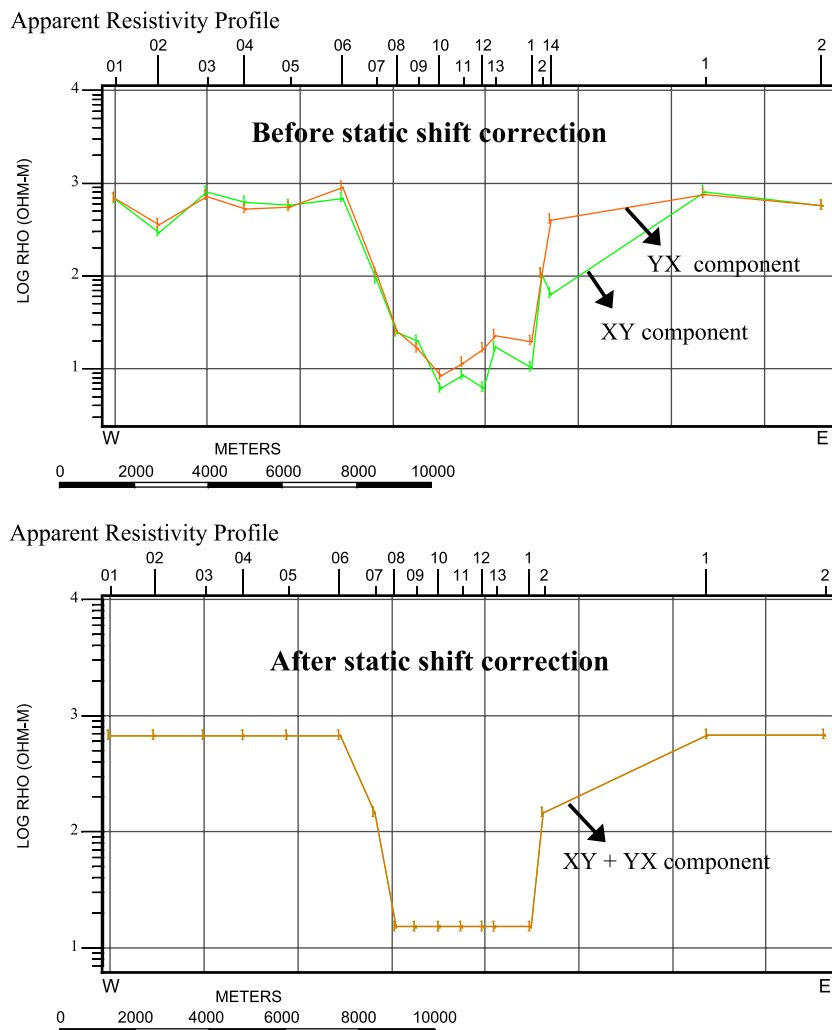

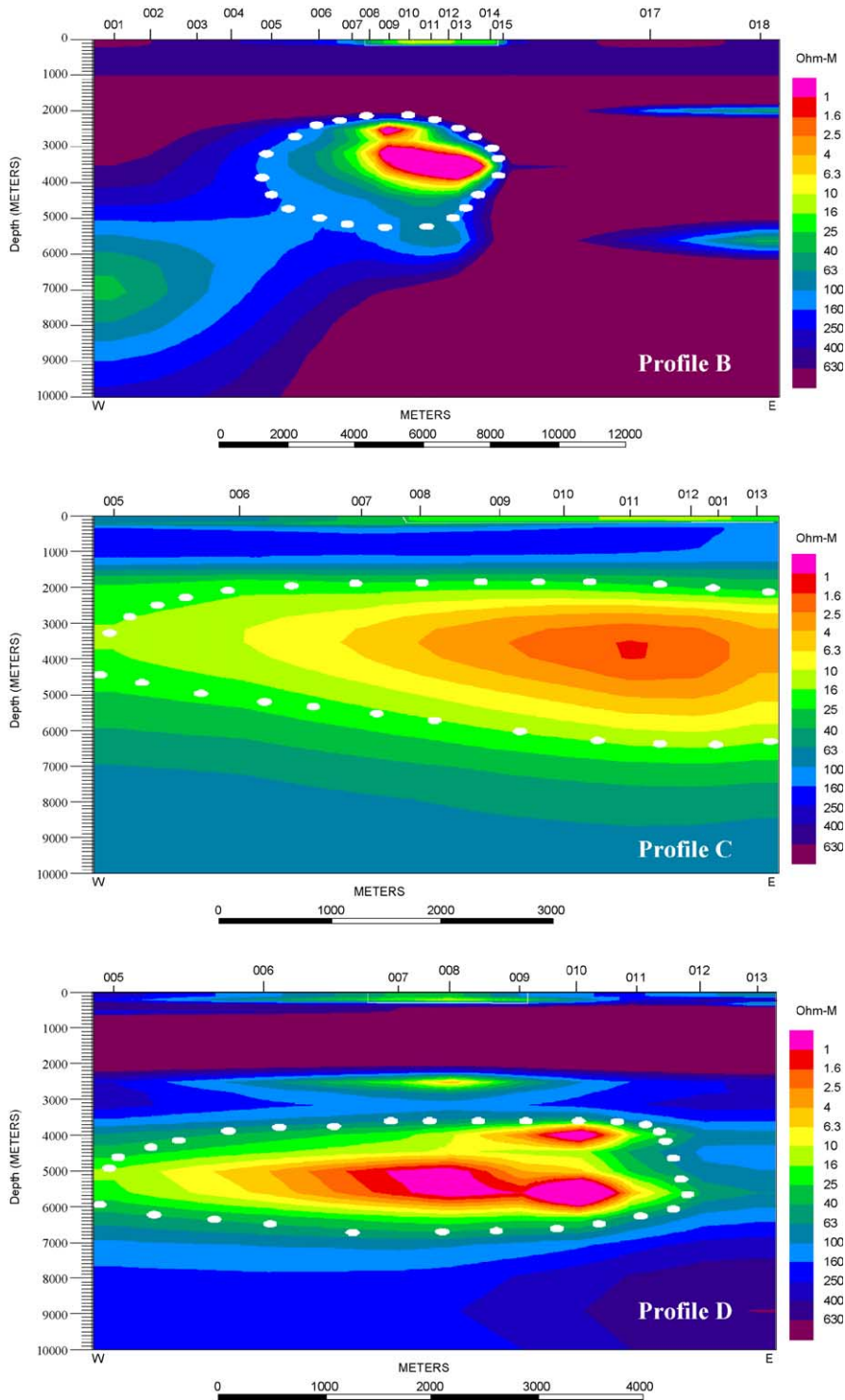Fig. 8. Apparent resistivity profile before and after static shift (Profile B).

Fig. 9. Two-dimensional models using RRI inversion along profiles B (top), C (middle) and D (bottom).
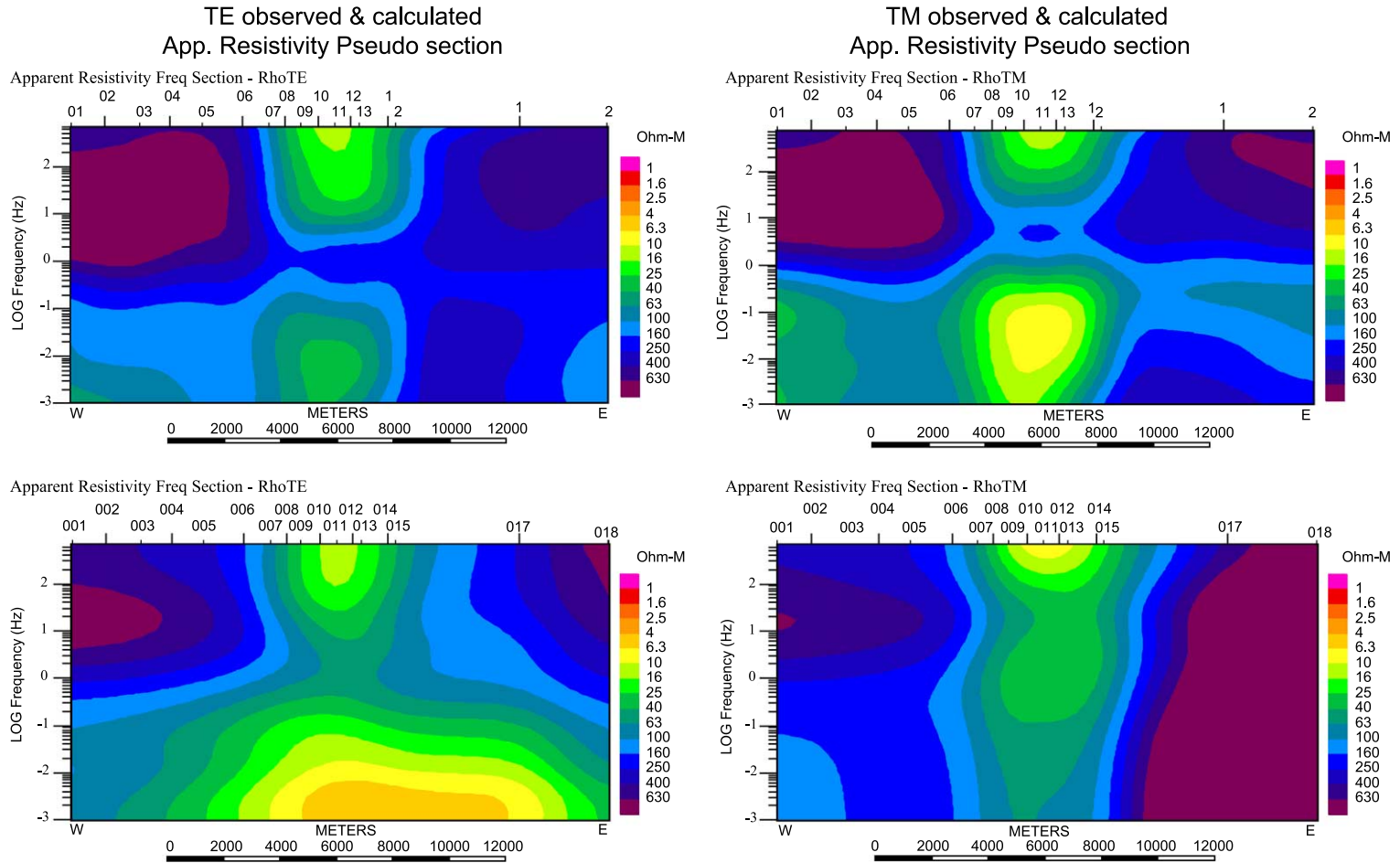
TE observed & calculated
App. Resistivity Pseudo section

TM observed & calculated
App. Resistivity Pseudo section

Fig. 10. Observed apparent resistivity (top) and phase (bottom) pseudo-sections: left, TE mode; right, TM mode.
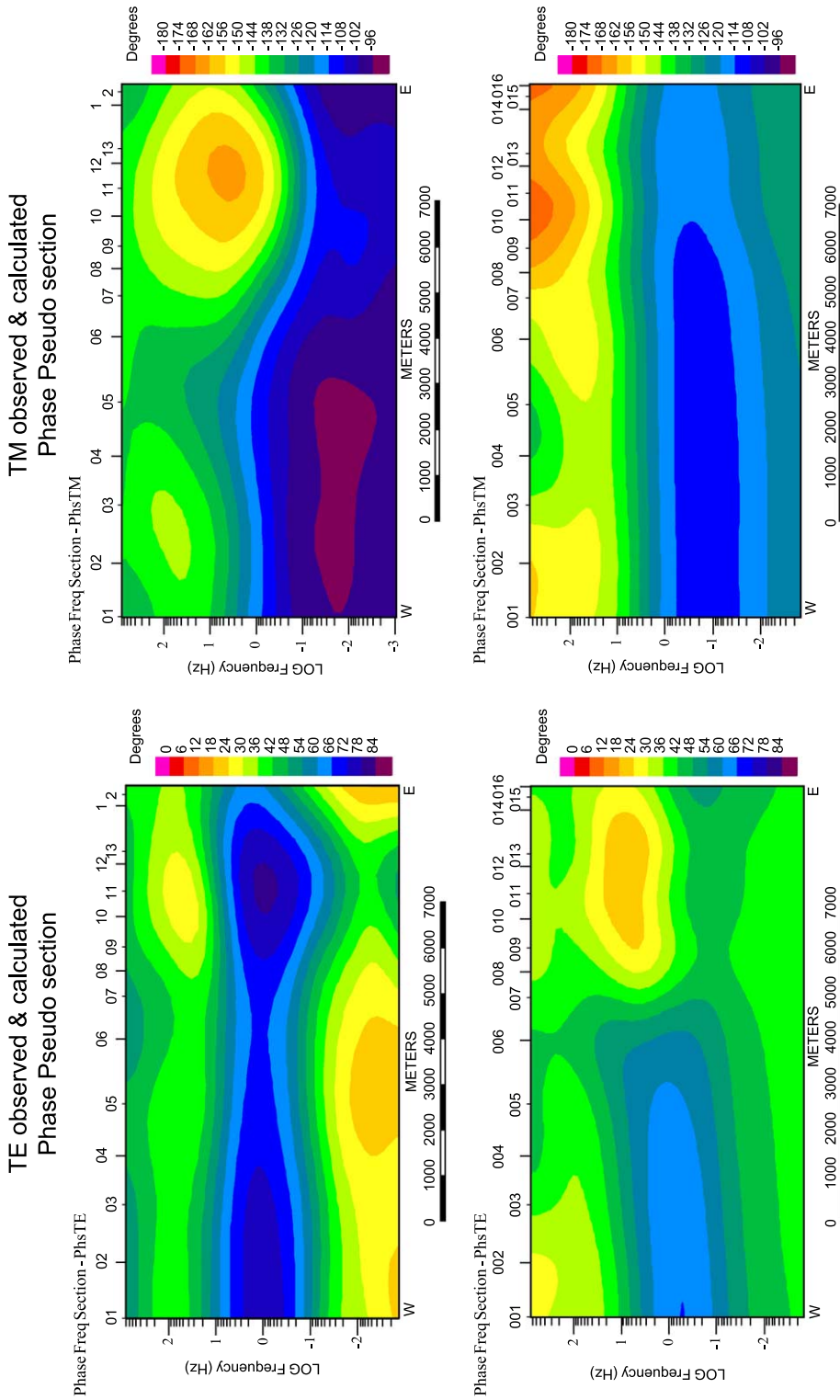
Fig. 10 (*continued*).

profile. This surface conductive region spreads about 4–5 km along the profile B and C, while it becomes narrow (~2 km) along the profile D. In addition to the shallow conductive zone, more importantly, an anomalous high conductive zone (<10 Ω m) is evident (marked with white dots in Fig. 9a, b and c) from 2D inversion results at a depth of about 1.5–2 km. The deeper anomalous conductive feature is clearly evident along all the three profiles with a width of about 5 km, indicating the larger dimension as compared to shallow conductive zone. Its depth extension is from 1.5 km to about 7 km. It seems to be shallow (1.5 km) along C profile. The observed apparent resistivity and phase pseudo section is compared with the computed apparent resistivity and phase pseudo section derived from RRI inversion model for TE and TM mode data along profile B (Fig. 10). The observed apparent resistivity and phase pseudo-sections (Fig. 10) indicate the presence of conductive features at higher frequency (>10 Hz) and lower frequency (<0.1 Hz) range in the middle of the profile.

Results along three profiles (Fig. 9) clearly demonstrate the presence of a confined conductive zone (<10 Ω m) within a comparatively resistive host rock. The spatial extent of the conductive zone is in accordance with the surface geothermal manifestations (Fig. 2). The surface geothermal activity is confined within two N–S trending faults, namely Kaigar Tso to the west and Zildat fault to the east and the depth extensions of these two faults could be a reason for the confinement of the deeper conductive zone. The magmatic activity that accompanied the closure of Tethyan Sea would have generated partial melts all along the collision zone. Such a mechanism could explain the anomalous conductive zone delineated in Puga valley by the present study. From MT modelling along a 150-km N–S profile in the region, Gokarn et al. (2002) attributed the conductive zone to ophiolite/partial melts. However, the existence of younger phases of granite emplacement along the valley (CEA, 1995) support the idea of partial melts as the cause for the high conductivity.

characterize the electrical structure. The results indicate the lateral and vertical variation in resistivity structure. The one-dimensional and two-dimensional inversion results reveal the occurrence of surficial conductive zone extending upto a depth of about 400 m underlain by a resistive structure. This surface conductive zone, present in the thermally manifested area, is in agreement with the low resistive regions mapped by earlier shallow electrical studies (Gupta et al., 1975; Singh et al., 1983; Mishra et al., 1996). The drilled borehole results from the area also confirmed the presence of top alluvium cover with varying thickness (15–200 m) underlain by breccia/bedrock (CEA, 1995). The surface conductive region centered in the anomalous part of the area could be possibly due to the combined effect of top alluvial cover filled with geothermal deposits and fractured breccia/bedrock in which hot water is circulating. This region may be acting as the geothermal reservoir in the area.

Furthermore, the MT inversion studies brought out the presence of anomalous conductive zone (<10 Ω m) at a depth of about 1.5–2 km. The boundaries of this conductive region have clearly been shown towards the east and the west and it seems to extend more towards the north as compared to south. The Puga area is located just south of the Indus suture zone; considered to be the collision of zone between the Indian and Asian plates. The presence of partial melts in the region is indicated from geophysical studies (Gokarn et al., 2002). This zone was subjected to intense basic to ultrabasic, plutonic to submarine volcanism of Cretaceous age and several phases of wide spread acid igneous activity from Upper cretaceous to Upper Tertiary times (Ravishankar et al., 1976). The above knowledge along with the high heat flow conditions (535.6 mW/m^2) prevailing in this area (Ravishankar et al., 1976) gives the possibility to think that these anomalous high conductive region is due to the presence of rock materials of high temperature (partial melts) present at deeper depths and may be acting as the source of geothermal activity in the area.

8. Summary and conclusion

The analysis and inversion of MT data acquired in Puga geothermal region has permitted us to

Acknowledgements

References

Arora, C.L., Singh, H., Das, L.K., Ghatak, T.K., Singh, R.P., Hakim, A., 1983. Geophysical exploration of the Puga Valley geothermal field, Ladakh District, Jammu and Kashmir State. Spec. Publ.-Geol. Surv. India 2, 631–646.

Baweja, B.K., 1967. A note on visit to the hot springs at Puga valley, Ladakh. Report of the Hot Spring Committee, Central Water and Power Commission, India (unpublished).

Berdichevsky, M.N., Dimitriev, V.I., 1976. Basic principles of interpretation of magnetotelluric sounding curves. In: Adam, A. (Ed.), Geolelectric and Geothermal Studies. KAPG Geophysical Monograph, Akademiai Kaido, Budapest, pp. 165–221.

Bostick, F.X., 1977. A simple and almost exact method of MT analysis (Abstract). Workshop on Electrical methods in Geothermal exploration, Snavford, U.T.

Cagniard, L., 1953. Basin theory of magnetotelluric method of geophysical prospecting. Geophysics 18, 605–635.

CEA, 1995. Status report of Puga geothermal assessment project district Ladakh (J and K). Technical report, Central Electricity Authority, New Delhi.

Chowdhury, A.N., Handa, B.K., Das, A.K., 1974. High lithium, rubidium and cesium contents of therma; spring water, spring sediments, and borax deposits in Puga valley, Kashmir, India. Geochem. J. 8, 61–65.

Constable, S.C., Parker, R.L., Constable, C.G., 1987. Occam's inversion: a practical algorithm for generating smooth models from e.m. sounding data. Geophysics 92, 289–300.

Geothermal Atlas of India, 1991. GSI Publ. 19.

Gokarn, S.G., Gupta, G., Rao, C.K., Selvaraj, C., 2002. Electrical structure across the Indus Tsangpo and Shyok suture zones in NW Himalaya using magnetotelluric Studies. Geophys. Res. Lett. 29 (8), 92-1–92-4.

Goldberg, S., Rotstein, Y., 1982. A simple form of presentation of magnetotelluric data using the Bostick transformation. Geophys. Prospect. 30, 211–216.

Groom, R.W., Baily, R.C., 1989. Decomposition of magnetotelluric impedance Tensors in the presence of local three-dimensional galvanic distortion. J. Geophys. Res. 94 (B2), 1913–1925.

Gupta, M.L., Singh, S.B., Rao, G.V., 1975. Study of D.C. resistivity in the Puga geothermal field, Himalayas, India. Abstr.-U.N. Symp. Dev. Use Geotherm. Res. 2, 1029–1036.

Gupta, M.L., Sharma, S.R., Drolia, R.K., Sigh, S.B., 1983. Subsurface thermal conditions of Puga valley hydrothermal field, Himalaya, India. J. Geophys. 54, 51–59.

Ingham, M.R., Hutton, V.R.S., 1982. Crustal and upper mantle structure in Scotland. Geophys. J. R. Astron. Soc. 69, 579–594.

Jangi, B.L., Bajaj, A.K., 1992. Report on the geothermal exploration in Puga valley, Ladakh District, Jammu and Kashmir, 1988–1989. GSI report (unpublished).

Jones, A.G., 1986. Parkinson's pointers potential perfidy! Geophys. J. R. Astron. Soc. 87, 1215–1224.

Jones, A.G., 1988. Static shift of magnetotelluric data and its removal in a sedimentary basin environment. Geophysics 53 (7), 967–978.

Livelybrooks, D.W., 1986. Modeling earth resistivity structure for MT data comparison of rotationally-invariant and conventional Earth response functions. (Abstract.). EOS Trans. Am. Geophys. Union 67, 918.

Marquardt, D.W., 1963. An algorithm for least-squares estimation of non-linear parameters. J. SIAM 11, 431–441.

Mishra, H.P., Ghatak, T.K., Rai, R.P., Mishra, R.K., 1996. Geoelectrical studies for demarcating geothermal reservoir in Puga Valley, Ladakh District, Jammu and Kashmir. Geothermal energy in India. Spec. Publ.-Ser. Geol. Surv. India 45, 65–68.

Parkinson, W.D., 1962. The influence of continents and oceans on geomagnetic variations. Geophys. J. R. Astron. Soc. 6, 441–449.

PROCMT User' guide, 1990. Offline processing software for magnetotelluric time series, Ver. 1.1. Metronix 75.

Raina, B.N., Nanda, M.M., Bhat, M.L., Mehrotra, P.C., Dhal, B.N., 1963. Report on the investigations of coal limestone borax, and sulphur deposits of Ladakh. Unpublished progress report. Geol. Surv. India.

Ranganayaki, R.P., 1984. An interpretive analysis of magnetotelluric data. Geophysics 49, 1730–1748.

Ravishankar, Padhi, R.N., Arora, C.L., Prakash, G., Thussu, J.L., Dua, K.J.S., 1976. Geothermal exploration of the Puga and Chumathang geothermal fields, Ladakh, India. 2nd Proc. on U. N. Symp. Dev. Use Geotherm. Res., vol. 1 pp. 245–258.

Singh, S.B., Drolia, R.K., Sharma, S.R., Gupta, M.L., 1983. Application of resistivity surveying to geothermal exploration in the Puga Valley, India. Geoexploration 21 (1), 1–11.

Smith, T.J., Booker, J.R., 1991. Rapid inversion of two and three dimensional magnetotelluric data. J. Geophys. Res. 96, 3905–3922.

Stodt, J.A., 1983. Noise analysis for conventional and remote reference magnetotellurics, PhD dissertation, Univ. of Utah, Logan.

Sule, P.O., Hutton, V.R.S., 1986. A broad-band magnetotelluric study in the south-eastern Scotland, data acquisition, analysis and one-dimensional modelling. Ann. Geophys., Ser. B Terr. Planet. Phys. 4, 145–156.

Virdi, N.S., Thakur, V.C., Kumar, S., 1977. Blueschist facies metamorphism from the Indus suture zone of Ladakh and its significance. Himal. Geol. 7, 479–482.

Vozoff, K., 1991. The magnetotelluric method. In: Nabighian, M.N. (Ed.), Electromagnetic Methods in Applied Geophysics, vol. 2. Society of Exploration Geophysicists, Tulsa, OK, pp. 641–707.